

Preequilibrium neutron emission from O + Al at 7.5 MeV/nucleon and 8.8 MeV/nucleonSabyasachi Paul,^{1,4} C. Sunil,¹ Sanjoy Pal,² V. Nanal,² V. Suman,¹ G. S. Sahoo,¹ A. Shanbhag,¹ S. P. Tripathy,^{1,4} T. Bandyopadhyay,^{1,4} M. Nandy,^{3,4,*} and A. K. Mohanty^{3,4}¹Health Physics Division, Bhabha Atomic Research Centre, Mumbai 400085, India²DNAP, Tata Institute of Fundamental Research, Mumbai 400005, India³Saha Institute of Nuclear Physics, 1/AF, Bidhannagar, Kolkata 700064, India⁴Homi Bhabha National Institute, Mumbai 400094, India

(Received 3 May 2017; published 10 October 2017)

The thick target neutron yield from a $^{16}\text{O}^{6+}$ beam on a thick ^{27}Al target at 120- and 142-MeV (7.5- and 8.8-MeV/nucleon, respectively) incident energies is presented and compared with theoretical calculations. The theoretical estimates for the yield of a high-energy neutron was obtained using a preequilibrium (PEQ) heavy-ion reaction model (HION), whereas that for the low-energy part was obtained using the standard evaporation models PACE4 and EMPIRE 3.2. In the present data a significant PEQ contribution, $\sim 2\%$ to 3% of the evaporation contribution, is observed even at projectile energies below 10 MeV/nucleon. The measured energy spectrum of neutrons for $E > 20$ MeV (the predominant PEQ region) is in good agreement with the PEQ model code HION.

DOI: [10.1103/PhysRevC.96.044607](https://doi.org/10.1103/PhysRevC.96.044607)**I. INTRODUCTION**

Thick target neutron yield (TTNY) measurements in heavy-ion interactions provide important data for numerous applications ranging from nuclear to material physics and medical applications to safety calculations [1–6]. A large number of experimental measurements and theoretical studies are available with ^{16}O as a projectile for different targets [7–14] covering a horizon of different kinds of analyses and investigations, but the study of TTNY is very sparse. Especially at the intermediate projectile energy range of 7–20 MeV/nucleon the data are very limited [15]. This energy range is crucial as it corresponds to a transition region between the equilibrium and the nonequilibrium emissions of particles. Below 5-MeV/nucleon projectile energies ([16] and references therein), particle emission through thermal equilibration and evaporation becomes the predominant deexcitation process. However, investigation of the lower-energy limit for initiation of nonequilibrium or preequilibrium (PEQ) emission processes [17–20] is still an open question even after few decades of rigorous research in this field. Blann [21–23] and Cline and Blann [24] carried out measurements with several projectiles (including ^{16}O) and claimed that no PEQ emission exists below 10 MeV/nucleon. On the other hand, there exists a number of experimental data and models [15,25–27], which bring the above results in question. For example, Nandy *et al.* have reported the presence of a significant amount of PEQ contribution with ^{16}O as a projectile on a thick Ta target even at 7.2 MeV/nucleon [15] (see also Ref. [28]). Therefore, the aim of the present paper is to find the PEQ contribution in the thick target neutron yield along with the yield distribution using the ^{16}O projectile with a lighter target nucleus (^{27}Al). The experiments were carried out at two different projectile energies, viz. 120 and 142 MeV corresponding to 7.5 and 8.8 MeV/nucleon, and an effort has

been made to estimate the PEQ neutron emissions from this (projectile + target, ^{43}Sc) system. A modified version of the in-house developed heavy-ion (HION) code [29,30] used by Nandy *et al.* [15] with some modification [31] was used to estimate the high-energy neutrons in the present paper. The assumptions made in the present version of the code are more realistic compared to the one used in Ref. [15] where the nucleon-nucleon (N-N) collision rate is determined from an empirical formalism. To overcome these shortcomings, a modified collision rate estimated from the spatial variation in the nucleon density distribution has been introduced in the improved model [30]. The energy and angular distributions of PEQ emitted neutrons were determined from two-body scattering kinematics [32–34] considering the fused system (^{43}Sc) as made of two different subsystems, a hot spot and a cold spot [29]. The particle emission probability was calculated from the spatial density-dependent collision rates in the fused systems based on: (i) a semiphenomenological approach [35,36] and (ii) relativistic mean field (RMF) theory [37,38]. The PEQ contribution in the present model extends until the fused composite system attains a thermodynamic equilibrium through N-N interactions. After attaining the thermal equilibration the emission probabilities are calculated through the Hauser-Feshbach evaporation formalism using the statistical model codes projection angular momentum coupled evaporation (PACE4) [39,40] and EMPIRE version 3.2 [41].

In the present paper an attempt has been made to estimate the emission neutron spectra from a heavy-ion nuclear reaction and to validate the experimental observations using the in-house developed PEQ formalism, the modified HION code at intermediate beam energies. The details of the experimental setup and data acquisition are described in the next section. Brief descriptions of the statistical model codes used in this paper and modifications in HION to study the effect of PEQ emission are presented in Sec. III. Section IV discusses the findings of the paper followed by the conclusion in Sec. V.

* maitreyee.nandy@saha.ac.in

II. EXPERIMENTAL SETUP

The experimental measurements were carried out at the Pelletron- Linac Facility, Mumbai, India. In the present paper $^{16}\text{O}^{6+}$ was bombarded on a thick ^{27}Al target (3 mm) at 120 and 142 MeV. The measured full width at half maximum of the beam was $\sim 0.8\text{--}1.0$ ns, inclusive of detector resolution. The produced neutron spectra were measured with the proton recoil scintillator detectors using the time-of-flight (ToF) technique. The ^{27}Al target was made in the form of a hemisphere of 40-mm diameter and 3-mm thickness to reduce the unwanted scattering and attenuation of the emitted neutrons [42,43]. The range of the projectiles in the thick aluminum target was estimated to be 110 and 142 μm for the above-mentioned energies using the SRIM code [44]. Thus, the complete removal of the projectile flux on the outer surface of the target assembly was ensured. The angular distributions and the TTTY were measured at five different angles with respect to the incoming projectile beam direction viz. $0^\circ, 30^\circ, 60^\circ, 90^\circ$, and 120° at two different distances using five (5×5)- cm^2 EJ301 (Scionix, Holland) recoil proton liquid scintillator detectors. For $0^\circ, 30^\circ$, and 60° the measurements were carried out at 2.0 m, and for 90° and 120° the distance was kept at 1.5 m from the target surface. The target-to-detector distance is reduced at backward angles as the contribution of high-energy neutrons is expected to be less than that at forward angles. In the ToF measurements, the longer distance ensures a better energy resolution at high emission neutron energies, i.e., a better resolution for the PEQ neutrons is expected due to the longer target-to-detector distance. A schematic of the experimental setup is explained in Fig. 1(a). The neutrons measured with this setup contain both direct neutrons and scattered ones from the structural as well as the shielding materials. So background corrections for the removal of the scattered components were carried out using the shadow bar technique. This was achieved with the help of two 30-cm-long cylindrical bars, one made of iron and the other made of high-density polyethylene, placed end to end between the target and the detector [as shown in Fig. 1(a)] to screen all the direct neutrons emitted from the reactions. The neutrons detected with this shadow bar in place are the scattered neutrons only. The background spectrum was measured at a single specified angle at a time. The background spectrum when subtracted from the total experimental spectrum (generated in the absence of a shadow bar) at that angle produces the net neutron distribution due to a heavy-ion nuclear reaction.

The electronic setup used in this experiment is shown schematically in Fig. 1(b). The neutrons were distinguished over the γ -ray photons by the zero crossover method using the anode output of the photomultiplier tube with the help of a four-channel pulse shape discriminator (PSD) module (MPD-4, Mesytec) and a constant fraction discriminator [(CFD), Canberra 454]. The initial trigger as a radio-frequency signal was obtained from the start signal. Each detector provides three sets of information, viz. TOF, pulse height (PH), and neutron-to- γ discrimination. So a total of 15 signals was acquired by an analog-to-digital converter (CAEN-V785) for offline analysis. For registering the signal pulses, a master gate with appropriate delay modules corresponding to different detectors was generated using the OR logic for the data acquisition from

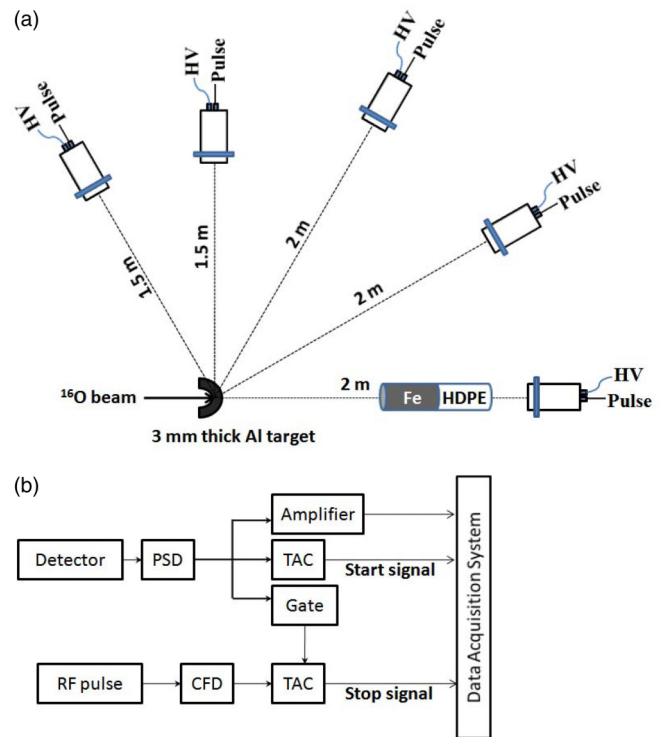


FIG. 1. The experimental setup for the $^{16}\text{O} + ^{27}\text{Al}$ system. (a) Schematic arrangement and (b) simplified block diagram of the electronic setup for the signal acquisition.

the CFD signals of all five detectors. The time-to-amplitude converter (TAC) provides the flight time of the neutrons which in turn gives the neutron energy. The module was calibrated using a TAC calibrator with a set of time signals of known width. The signals for the n - γ separation from the PH versus PSD and corresponding PSD versus ToF-TAC outputs are presented in Figs. 2(a) and 2(b), respectively, for the $^{16}\text{O}^{6+} + ^{27}\text{Al}$ system. Figure 2(b) corresponds to the two bunches of the chopped beam. The time difference between the two γ lines is 107.3 ns, and the neutrons and γ are found to clearly be separated. The neutron bunch between the two γ lines is basically the neutrons generated by the bombardment of $^{16}\text{O}^{6+}$ on the thick ^{27}Al target, the left γ line represents the flash of a projectile on the target, and the neutrons generated from the reaction were acquired by the proton recoil detectors until the second bunch of the projectile hits the target, which is signaled by the second flash of the γ line.

The acquired data then are analyzed offline using the Linux advanced multiparameter system [45] to obtain the neutron spectra from the ToF information. From the measured data the neutron yield per projectile is determined at different angles, corrected for background, solid angle, and intrinsic efficiency of the detectors. The detector intrinsic efficiency was obtained from Monte Carlo calculation [42] and assumed to be the same for all five detectors mounted at different angles. A more detailed description of the measurement technique, associated time energy uncertainties, and systematic errors can be found in Ref. [42].

The neutron energy spectra for both energies after the efficiency correction has been presented in Fig. 3. The circular dots

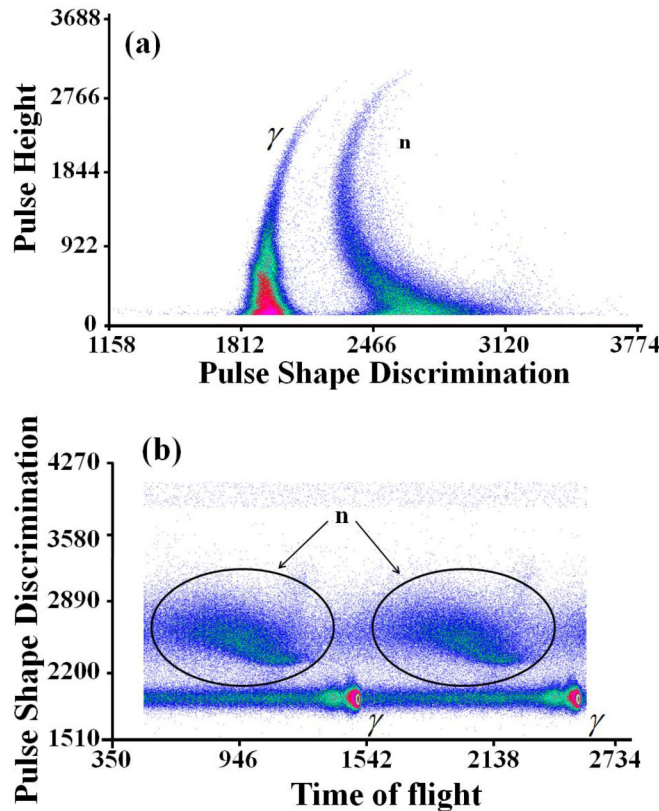


FIG. 2. A typical experimental output of the n - γ separation (a) pulse height and PSD spectra and (b) contour plot of PSD and TOF spectra for the $^{16}\text{O} + ^{27}\text{Al}$ system.

represent the emitted neutrons produced from bombardment of 120 MeV, and the open circles represent the emitted neutrons for the 142-MeV ^{16}O beam on a thick Al target. The data points in these figures represent the experimental neutron yield per incident projectile in a unit solid angle in an energy bin of 1 MeV. The error bars associated with the measurements are

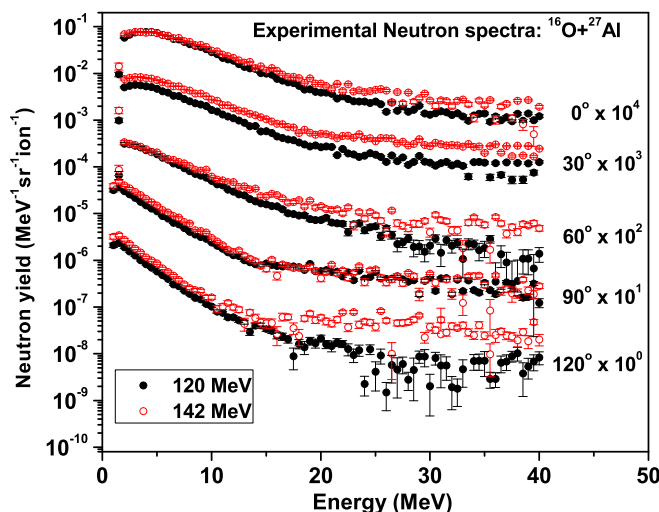


FIG. 3. A comparison between the experimental neutron yield at 120 and 142 MeV.

statistical in nature. The low-energy limit in the measured data results from the limitation of the experimental setup aimed at a better resolution for higher-energy neutrons.

III. REACTION MODEL CALCULATIONS

A. Equilibrium emissions

The objective of the paper is to obtain the experimental neutron yields from the $^{16}\text{O}^{6+} + ^{27}\text{Al}$ system at different energies and to estimate the contribution of PEQ neutrons. So in order to achieve that, statistical model calculations were carried out to estimate the emission from the equilibrated compound nuclei at these energies. In this paper two different nuclear reaction model codes, EMPIRE version 3.2 and PACE4 were used for estimating the evaporation neutrons.

1. PACE4

The PACE code is a modified version of the Hillman-Eyal evaporation code (JULIAN). It calculates compound nuclear emission considering angular momentum coupling at each stage of the deexcitation process. A Monte Carlo random sampling is used, and all possible decay channels are considered with proper weightage [39]. The formation of a composite nucleus is calculated using the Bass model. The composite system deexcites solely by evaporation residues determined by fission barrier height and level densities. The mode of deexcitation is calculated from the excited compound nucleus after normalizing the initial spin distributions.

2. EMPIRE 3.2

EMPIRE is an adaptive set of nuclear reaction codes. It uses various nuclear models for different kinds of projectiles with a largely varying energy range [41]. But in the case of heavy-ion reactions the model predictions deteriorate above an energy of 8 MeV/nucleon. In the present version of the code, for estimating the neutron emission after thermal equilibration, compound nucleus decay is described by the Hauser-Feshbach theory. Angular momentum and parity coupling are considered through l -dependent transmission coefficients. The Hofmann, Richert, Teple, and Weidenmuller model is used for establishing the correlation between entrance and exit channels for elastic scattering. In the present paper, the neutron emissions were calculated using the dynamic EMPIRE-specific level-density approach. This uses the superfluid model below a critical excitation energy and the Fermi-gas model at higher energies for a proper accounting of the spin-dependent rotation-induced deformation of the nucleus at higher energies.

B. Preequilibrium model calculation

The statistical model codes fail to reproduce the entire emission neutron spectra obtained from experiments for incoming projectile energies of 7 to 8 MeV/nucleon or beyond. Primarily the statistical model codes underestimate the higher-energy emission neutrons. This is mainly because of the presence of PEQ neutrons which are emitted before thermodynamic equilibrium between the nucleons was attained in the composite system. In the present paper, the

projectile energies were chosen close to this energy range to determine the presence of PEQ neutrons if any and to estimate the contribution of this component in the total experimental neutron yield. The PEQ contribution has been estimated using the in-house developed heavy-ion code (HION) [29,30], based on the nucleon-nucleon scattering interactions until the excited composite system attains a thermodynamic equilibrium. The interaction of nucleons in the hot spot will generate more energetic particles in the progressive stages of the interactions through creation, annihilation, or redistribution of the excited nucleons and corresponding holes. These excited nucleons and holes are collectively known as exciton pairs. Energy-angle distribution of the nucleons due to hot spot scattering is calculated from the two-body scattering kinematics after incorporating the effect of nuclear excitation. Emission of nucleons and light particles can take place from the hot spot before the thermal equilibrium is attained. The second type of interaction between particles in the hot spot with those in the cold spot leads to the creation of excited particle-hole pairs. Energy-angle distribution of these excited particles can be estimated through the Kikuchi-Kawai scattering kinematics. Finally the energy-angle distribution of PEQ neutron emission from heavy-ion reactions was estimated through the emission probability calculated from the density-dependent nucleon-nucleon collision rates. The details of the model and the two-body scattering kinematics related to the model can be found elsewhere [32–34]. In the present paper, the nucleon-nucleon collision rates in the composite system (^{43}Sc) were estimated from the spatial nucleon density distribution calculated using the semiphenomenological approach [35,36], and RMF theory [37,38] and only the neutron emission is estimated from the composite system.

C. Thick target yield

In order to determine the energy-angle distribution of emitted neutrons from the thick target, it was assumed that inside the target the projectile interacts at a continuously degrading energy. The thick target neutron spectra are effectively a sum of all the neutron distributions at these different projectile energies folded by the fusion cross section of the projectile in the target at respective energies. The details of the methodology of the conversion of the thin target neutron emission to a thick target emission spectrum can be found in Ref. [15].

IV. RESULTS AND DISCUSSION

The comparisons between the experimental neutron yields with evaporation estimates from the statistical model codes PACE and EMPIRE are presented in Figs. 4(a) and 4(b) for beam energies of 120 and 142 MeV, respectively. All model calculations were performed in a laboratory frame. In order to estimate the thick target neutron yield from the thin target contributions, the energy decrement has been chosen in steps of 5 MeV in each of the thin slices of the target medium starting from the incident energy until the Coulomb barrier. The solid circles correspond to the experimental measurements with the associated experimental and statistical uncertainties

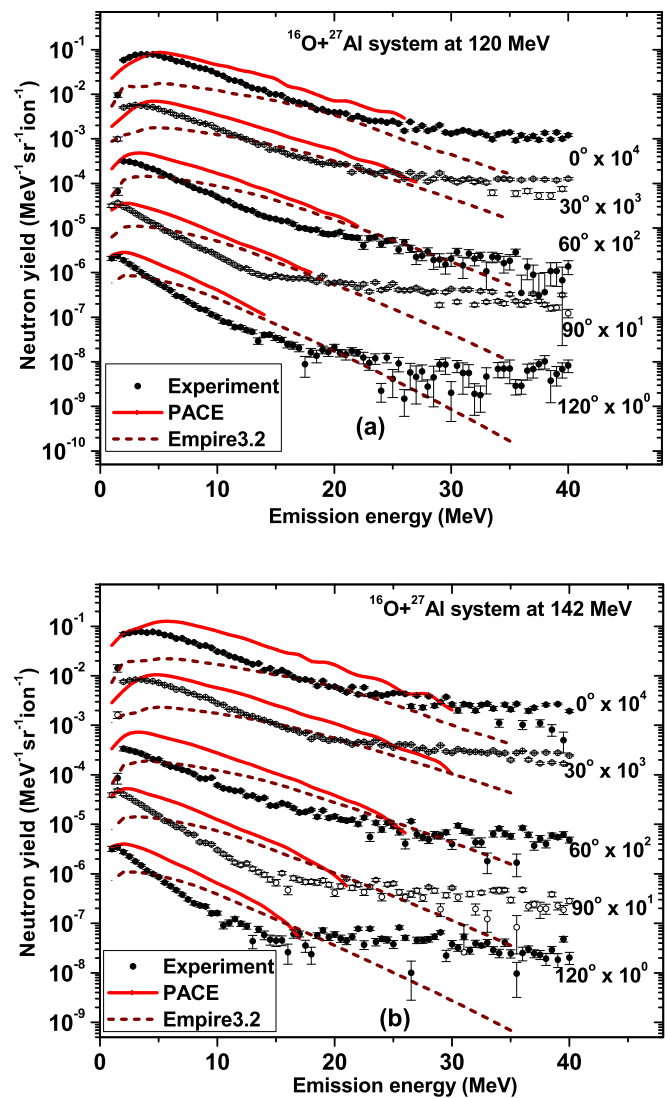


FIG. 4. Comparison of the experimental neutron yield with evaporation estimates from the statistical model codes PACE and EMPIRE at (a) 120 MeV and (b) 142 MeV, respectively. The spectra for 0° , 30° , 60° , 90° , and 120° are multiplied with 10^n with n being 4, 3, 2, 1, and 0, respectively.

represented as vertical error bars. The solid and the dotted lines represent the thick target neutron yields estimated from PACE4 and EMPIRE 3.2, respectively. Both figures clearly depict that, at lower neutron energies, the statistical model code results are comparable with the experimental observations. The slope of the neutron energy distribution is fairly reproduced by the PACE calculations up to 25 MeV at 0° and 30° and up to 20 MeV at 60° . At backward angles the agreement shifts to lower energies. The PACE estimated numbers show a better corroboration with the measured data at low neutron energies, and the EMPIRE results give a better estimate at intermediate neutron energies at 0° and 30° for both beam energies.

The PACE calculations overpredict the measured evaporation neutron yield at all angles as shown in Fig. 4. The PACE results also give higher neutron yield compared to those obtained from EMPIRE 3.2, which may be attributed

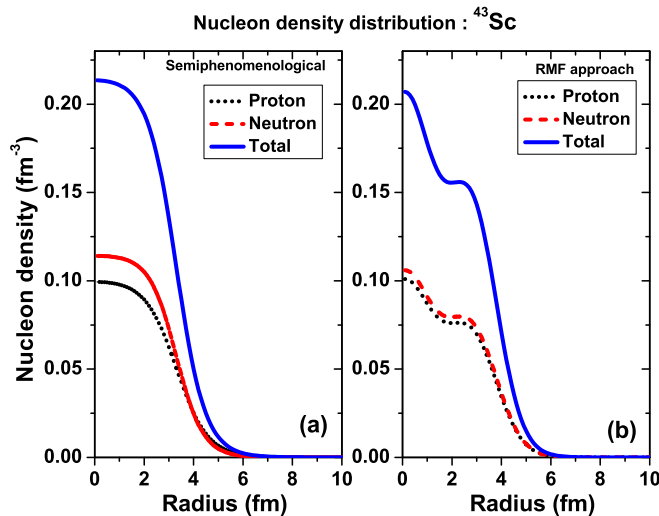


FIG. 5. Nucleon density distribution for the compound nucleus $^{43}\text{Sc}(^{16}\text{O}+^{27}\text{Al})$ system using (a) the semiphenomenological and (b) the RMF approaches.

to the variation in emission probabilities resulting from the choice of level-density parameters. In both energies, the PACE calculations were trimmed at higher emission neutron energies considering a sharp decrease in the population of neutrons leading to large calculation uncertainties. It has been observed from Figs. 4(a) and 4(b) that the measured TTNY is underpredicted by both models at higher emission energy. The discrepancy is highest at 0° and decreases at wider angles. This clearly indicates the presence of a significant PEQ contribution in the experimental spectra along with the usual evaporation neutrons.

In order to account for the higher neutron yields, an attempt has been made to include the contribution of the PEQ neutrons at higher emission energies. The PEQ contribution theoretically is obtained using the preequilibrium model HION [29,31]. In the present paper the spatial nucleon density distribution in the composite nucleus ^{43}Sc is determined from the semiphenomenological approach of Gambhir and Patil [35,36] and the RMF theory [37,38]. Moreover, in the present paper with the incident energy being less than 10 MeV/nucleon, only single preequilibrium neutron emission has been considered to estimate the PEQ neutron yield from HION. The nucleon density profile of the composite system (^{43}Sc) from the semiphenomenological approach and from RMF theory is shown in Fig. 5.

Figure 5(a) shows that the density remains almost constant up to 2.5 fm and then sharply falls and reduces to almost zero by 6 fm. The central neutron density is 0.11 fm^{-3} , and the corresponding proton density is 0.1 fm^{-3} . From Fig. 5(b) it is observed that the central neutron density is $\sim 0.105\text{ fm}^{-3}$ and the central proton density is $\sim 0.1\text{ fm}^{-3}$. We have calculated the collision rates and the corresponding emission probabilities using the proton and neutron density distributions obtained from the two approaches. The details of the collision rate and emission probability calculations can be found elsewhere [31]. Neutron energy-angle distributions for both beam energies were calculated from HION using the emission probabilities

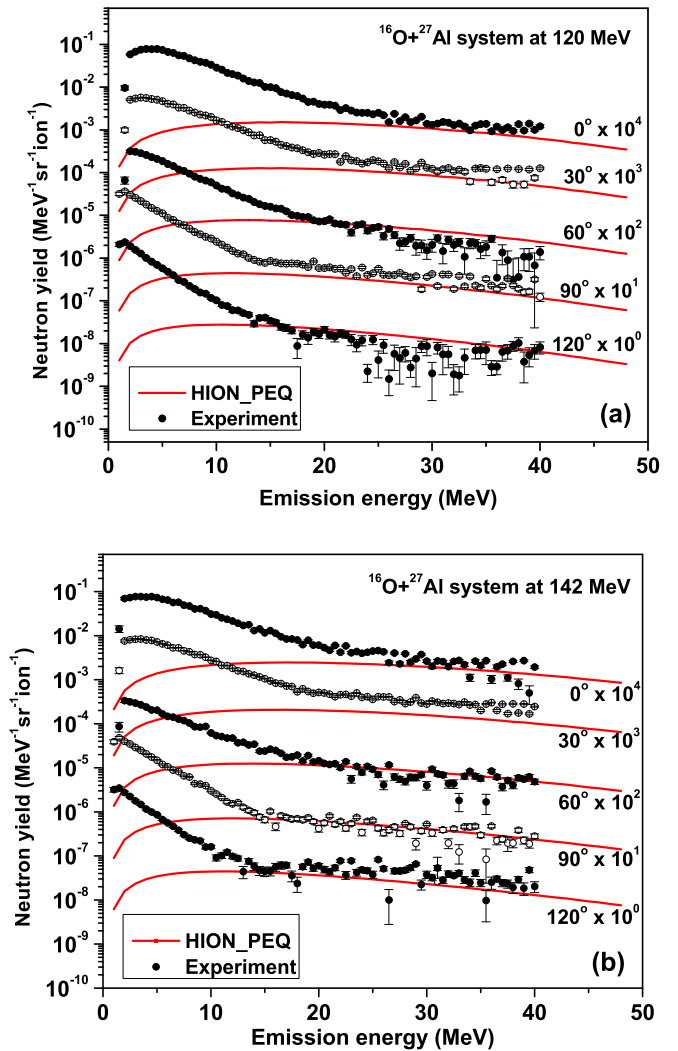


FIG. 6. Comparison of experimental neutron yield with HION estimated PEQ contribution at (a) 120 MeV and (b) 142 MeV.

obtained from the semiphenomenological approach and RMF theory. It was observed that for 142 and 120 MeV at forward angles the maximum variation in neutron emission obtained from the two formalisms is $\sim 5\%$. As in the case of a thick target where the total yield obtained is the weighted sum of neutron yields from gradually decreasing energies, the PEQ contribution gradually decreases, and the variation in the total yield is lower. So in this paper, we have used the collision rates and emission probabilities obtained from the semiphenomenological approach. The experimentally obtained neutron spectra and the corresponding PEQ neutron yields at different angles estimated from the HION code are presented in Figs. 6(a) and 6(b) for the 120- and 142-MeV $^{16}\text{O}^{6+}$ projectile beams, respectively, on a thick ^{27}Al target. For comparison in a single frame, the measured as well as the HION estimated neutron yields were multiplied with 10^n , where n is 4, 3, 2, 1, and 0 for $0^\circ, 30^\circ, 60^\circ, 90^\circ$, and 120° , respectively. The circular dots with error bars represent the experimental measurements, and the solid line represents the HION estimates. The results show a close agreement

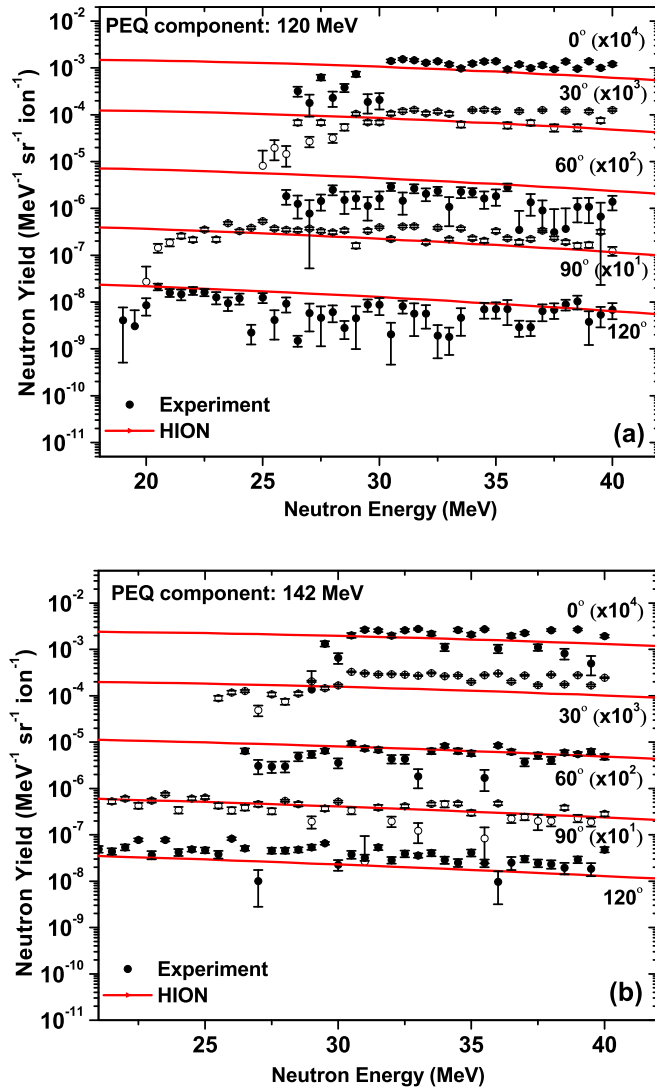


FIG. 7. Comparison of the evaporation subtracted experimental spectra with HION estimates at (a) 120 MeV and (b) 142 MeV.

of the experiment with the theoretical estimates at higher emission energies. At forward angles, the PEQ contribution is higher compared to the backward angles as is evident from Fig. 6.

For an estimate of the PEQ contribution from experiment, the evaporation contributions estimated from the PACE code for both 120 and 142 MeV were subtracted from the experimental spectra above 25-MeV emission energy at 0° , 30° , and 60° and above 20-MeV emission energy at 90° and 120° . The subtracted contributions are presented in Fig. 7 for 120 and 142 MeV along with the calculations from HION for a closer look at the PEQ contribution of the emission neutrons. The resultant distribution confirms a PEQ contribution in the experimental thick target neutron yield both at 120 and 142 MeV. Moreover, the HION calculations have reproduced the measured PEQ contribution at all angles. From the TTTY data and HION calculations, it has been found that for 142- and 120-MeV beam energies the PEQ contributions at the 0° emis-

sion angle are 3.3% and 2.3%, respectively, of the evaporation contribution. At wider angles the PEQ contribution gradually reduces.

V. CONCLUSION

In the present paper the measured thick target neutron yield from the bombardment of $^{16}\text{O}^{+6}$ on a thick ^{27}Al target at two different energies viz., 120 MeV (7.5 MeV/nucleon) and 142 MeV (8.8 MeV/nucleon) is presented. The measured data have been analyzed in the framework of evaporation and the PEQ reaction models PACE4, EMPIRE 3.2, and HION, respectively. An attempt has been made to theoretically estimate the contribution of equilibrium-to-preequilibrium neutron emissions and to validate the PEQ reaction model HION. In the theoretical estimation of PEQ emission from the HION model, the spatial nucleon density distribution of the composite (^{43}Sc) system was used to calculate the collision rate and emission probability. As the projectile energy is less than 10 MeV/nucleon [31], only single-particle PEQ emission has been considered to estimate the neutron yield. Comparison of the experimental data with the model calculations showed that the modified version of the HION code can predict the PEQ contribution fairly well. Our calculations showed that, for the 7.5- and 8.8-MeV/nucleon cases, the PEQ contributions at 0° were found to be 2.3% and 3.3%, respectively, of the evaporation contribution. This clearly indicates the presence of PEQ emissions at energies below 10 MeV/nucleon. It has also been observed in this paper that the HION model fairly well predicts the PEQ contribution in the energy range considered. In our earlier work [31] we have shown that the model could handle PEQ emissions from heavy-ion reactions in the energy range from 10 to 30 MeV/nucleon for large mass number composite systems with the incorporation of multiple preequilibrium and relativistic mean-field effects. Similarly, this paper establishes that, employing similar formalism with even less mathematical complexities viz., using a semiphenomenological approach for nucleon density distributions with single-particle PEQ emission formalism, the experimental observations can be reproduced theoretically even below 10 MeV/nucleon with relatively low mass number composite systems as well.

ACKNOWLEDGMENTS

The authors sincerely thank Dr. R. M. Tripathi, Head, Health Physics Division and Dr. K. S. Pradeepkumar, Associate Director, Health, Safety & Environment Group, BARC for the inspiration in carrying out these studies. The authors wish to extend their sincere thanks to all the staff members of TIFR-BARC Pelletron Facility, DNAP, and TIFR for the beam line setup, all help, and support during the entire course of the experiment. The authors are grateful to Dr. P. K. Sarkar, Manipal Centre for Natural Sciences, Manipal University and Ex-BARC, Mumbai and Professor Y. K. Gambhir, IIT, Mumbai for their fruitful academic discussions and suggestions. One of the authors, M.N., acknowledges support from the XIIth Plan Projects BARD, SINP, and DAE for financial and infrastructural support in carrying out the work.

- [1] P. K. Sarkar, T. Bandyopadhyay, G. Muthukrishnan, and S. Ghosh, *Phys. Rev. C* **43**, 1855 (1991).
- [2] W. B. Howard, S. M. Grimes, T. N. Massey, S. I. Al-Quraishi, D. K. Jacobs, C. E. Brient, and J. C. Yanch, *Nucl. Sci. Eng.* **138**, 145 (2001).
- [3] U. Amaldi and G. Kraft, *J. Radiat. Res.* **48**, A27 (2007).
- [4] T. Nakamura, *Radiat. Prot. Environ.* **35**, 111 (2012).
- [5] F. Castillo, G. Espinosa, J. I. Golzarri, D. Osorio, J. Rangel, P. G. Reyes, and J. J. E. Herrera, *Radiat. Meas.* **50**, 71 (2013).
- [6] S. Agosteo, A. Mereghetti, E. Sagiab, and M. Silari, *Nucl. Instrum. Methods Phys. Res., Sect. B* **319**, 154 (2014).
- [7] D. J. Hinde, W. Pan, A. C. Berriman, R. D. Butt, M. Dasgupta, C. R. Morton, and J. O. Newton, *Phys. Rev. C* **62**, 024615 (2000).
- [8] M. Trotta, A. M. Stefanini, S. Beghini *et al.*, *Eur. Phys. J. A* **25**, 615 (2005).
- [9] M. Dasgupta, D. J. Hinde, A. Diaz-Torres, B. Bouriquet, C. I. Low, G. J. Milburn, and J. O. Newton, *Phys. Rev. Lett.* **99**, 192701 (2007).
- [10] P. P. Singh, B. P. Singh, M. K. Sharma, Unnati, D. P. Singh, R. Prasad, R. Kumar, and K. S. Golda, *Phys. Rev. C* **77**, 014607 (2008).
- [11] R. Tripathi, K. Sudarshan, S. K. Sharma, K. Ramachandran, A. V. R. Reddy, P. K. Pujari, and A. Goswami, *Phys. Rev. C* **79**, 064607 (2009).
- [12] U. Gupta, P. P. Singh, D. P. Singh, M. K. Sharma, A. Yadav, R. Kumar, S. Gupta, H. D. Bhardwaj, B. P. Singh, and R. Prasad, *Phys. Rev. C* **80**, 024613 (2009).
- [13] E. Prasad, K. M. Varier, N. Madhavan, S. Nath, J. Gehlot, S. Kalkal, J. Sadhukhan, G. Mohanto, P. Sugathan, A. Jhingan, B. R. S. Babu, T. Varughese, K. S. Golda, B. P. Ajith Kumar, B. Satheesh, S. Pal, R. Singh, A. K. Sinha, and S. Kailas, *Phys. Rev. C* **84**, 064606 (2011).
- [14] K. Kumar, T. Ahmad, S. Ali, I. A. Rizvi, A. Agarwal, R. Kumar, K. S. Golda, and A. K. Chaubey, *Phys. Rev. C* **87**, 044608 (2013).
- [15] M. Nandy, T. Bandyopadhyay, and P. K. Sarkar, *Phys. Rev. C* **63**, 034610 (2001).
- [16] T. C. Awes, G. Poggi, C. K. Gelbke, B. B. Back, B. G. Glagola, H. Breuer, and V. E. Viola, Jr., *Phys. Rev. C* **24**, 89 (1981).
- [17] J. J. Griffin, *Phys. Rev. Lett.* **17**, 478 (1966).
- [18] M. Blann and A. Mignerey, *Nucl. Phys.* **A186**, 245 (1972).
- [19] P. E. Hodgson, G. M. Field, H. Gruppelaar, and P. Nagel, *Radiation Eff.* **95**, 27 (1986).
- [20] M. B. Chadwick, R. Bonetti, and P. E. Hodgson, *J. Phys. G: Nucl. Part. Phys.* **15**, 237 (1989).
- [21] M. Blann, *Phys. Rev. C* **23**, 205 (1981).
- [22] M. Blann, *Phys. Rev. C* **31**, 1245 (1985).
- [23] M. Blann, *Phys. Rev. Lett.* **27**, 337 (1971); **27**, 700(E) (1971); **27**, 1550(E) (1971).
- [24] C. K. Cline and M. Blann, *Nucl. Phys. A* **172**, 225 (1971).
- [25] T. Otsuka and K. Harada, *Phys. Lett. B* **121**, 106 (1983).
- [26] O. V. Fotina, D. O. Eremenko, Y. L. Parfenova *et al.*, *Int. J. Mod. Phys. E* **19**, 1134 (2010).
- [27] J. Wilczynski *et al.*, *Nucl. Phys.* **A373**, 109 (1982).
- [28] K. A. Geoffroy, D. G. Sarantites, M. L. Halbert, D. C. Hensley, R. A. Dayras, and J. H. Barker, *Phys. Rev. Lett.* **43**, 1303 (1979).
- [29] M. Nandy, S. Ghosh, and P. K. Sarkar, *Phys. Rev. C* **60**, 044607 (1999).
- [30] P. K. Sarkar and M. Nandy, *Phys. Rev. E* **61**, 7161 (2000).
- [31] S. Paul, M. Nandy, A. K. Mohanty, and Y. K. Gambhir, *Phys. Rev. C* **94**, 034607 (2016).
- [32] A. De, T. Shibata, and H. Ejiri, *Phys. Rev. C* **45**, 774 (1992).
- [33] A. De, S. Ray, and S. K. Ghosh, *J. Phys. G: Nucl. Part. Phys.* **13**, 1047 (1987).
- [34] A. De, S. Ray, and S. K. Ghosh, *J. Phys. G: Nucl. Part. Phys.* **11**, L79 (1985).
- [35] Y. K. Gambhir and S. H. Patil, *Z. Phys. A: At. Nucl.* **321**, 161 (1985).
- [36] Y. K. Gambhir and S. H. Patil, *Z. Physik A* **324**, 9 (1986).
- [37] Y. K. Gambhir, P. Ring and A. Thimet, *Ann. Phys.* **198**, 132 (1990).
- [38] P. Ring, *Prog. Part. Nucl. Phys.* **37**, 193 (1996).
- [39] A. Gavron, *Phys. Rev. C* **21**, 230 (1980).
- [40] O. B. Tarasov and D. Bazin, *Nucl. Instrum. Methods Phys. Res., Sect. B* **204**, 174 (2003).
- [41] M. Herman, R. Capote, B. V. Carlson *et al.*, *Nucl. Data Sheets* **108**, 2655 (2007).
- [42] V. Suman, C. Sunil, Soumya Nair, S. Paul *et al.*, *Nucl. Instrum. Methods Phys. Res., Sect. A* **800**, 29 (2015).
- [43] C. Sunil, T. Bandyopadhyay, M. Nandy *et al.*, *Nucl. Instrum. Methods Phys. Res., Sect. A* **721**, 21 (2013).
- [44] J. F. Ziegler, M. D. Ziegler, and J. P. Biersack, *Nucl. Instrum. Methods Phys. Res., Sect. B* **268**, 1818 (2010).
- [45] A. Chatterjee (private communication); <http://www.tifr.res.in/~pell/lamps.html>